

**N65-21666**  
(ACCESSION NUMBER)  
54  
(PAGES)  
1MX-55203  
(NASA CR OR TMX OR AD NUMBER)

(THRU)  
1  
(CODE)  
07  
(CATEGORY)

*NASA TMX-55203*

## LOW NOISE TUNNEL DIODE RECEIVERS FOR SATELLITE APPLICATION

GPO PRICE \$ \_\_\_\_\_

OTS PRICE(S) \$ \_\_\_\_\_

Hard copy (HC) \$3.10Microfiche (MF) .50

FEBRUARY 17, 1965



— GODDARD SPACE FLIGHT CENTER —  
GREENBELT, MARYLAND

**CASE FILE COPY**

LOW NOISE TUNNEL DIODE RECEIVERS  
FOR SATELLITE APPLICATION

by

John B. Williams, Joseph Deskevich,  
and Michael A. Galli

February 17, 1965

Goddard Space Flight Center  
Greenbelt, Md.

## CONTENTS

Abstract .....	v
INTRODUCTION .....	1
REDUCTION OF SATELLITE FRONT-END NOISE AS A MEANS OF REDUCING GROUND TRANSMITTED POWER .....	2
COMPARISON OF LOW NOISE RF AMPLIFIERS FOR SPACE- CRAFT APPLICATION .....	5
Traveling-Wave Tube .....	5
Parametric Amplifiers .....	7
Masers .....	8
Tunnel Diode Amplifier .....	10
Comparison of Low-Noise Amplifiers .....	11
DESCRIPTION OF THE SIX LOW NOISE RECEIVERS .....	12
TUNNEL DIODE RECEIVER PERFORMANCE TESTS .....	16
Tunnel Diode Receiver Saturation Level .....	16
Tunnel Diode Receiver Broadband Noise Figure .....	19
Tunnel Diode Receiver Small Signal Gain vs Frequency .....	22
ANALYSIS OF TEST RESULTS .....	23
Tests at +25°C .....	23
Temperature Tests .....	26
APPLICATION OF TUNNEL DIODES TO A SATELLITE SYSTEM .....	27
ACKNOWLEDGMENT .....	32
Appendix A—The Tunnel Diode as a Circuit Element .....	33
Appendix B—The Effect of Temperature Variation on Ferrite Circulator Operation .....	45

LOW NOISE TUNNEL DIODE RECEIVERS  
FOR SATELLITE APPLICATION

by .

John B. Williams, Joseph Deskevich  
and Michael A. Galli

Abstract

21666

This report covers a study program conducted to investigate the feasibility of using a tunnel diode receiver to provide improved characteristics for the front end of a communication satellite transponder. Pre-amplification at a lower noise figure can be provided to establish optimum sensitivity and efficiency for the receiving section of the transponder; this in turn can allow a reduction in ground transmitted power. Analysis and measured performance are presented with emphasis on saturation, noise, and small signal gain vs. frequency. A comparison of the tunnel diode receiver to other low noise amplification devices for satellite application is also included as is an analysis of its possible use with the Applications Technology Satellite. This effort was performed under a Communications Supporting Research Task entitled, "Low Noise Receiver Techniques for Active Communication Satellites." No further studies are being performed with respect to this task.

*Author*

## LOW NOISE TUNNEL DIODE RECEIVERS FOR SATELLITE APPLICATION

### INTRODUCTION

The ability to transmit very large amounts of signal power from a ground station has been one of the lesser problems facing designers of communication satellite transponders of the Telstar, Relay and Syncom types. In each case, very large diameter transmitting antennas and transmitting tubes of kilowatt outputs were available for the ground stations. The cost of the transmitting equipment, though a consideration, was not the limiting factor.

After the initial satellite experiments which prove the feasibility of communications via an active communication satellite, the system designer quite naturally strives to improve system performance by refinement of previously used techniques and by the introduction of new techniques and components. One immediate improvement in system performance that is sought is the reduction of the required ground transmitted power. This improvement is sought for three reasons: 1) It is desirable to operate the entire system as efficiently and economically as possible. If the addition of a simple component to the satellite; which adds no noticeable complexity to the system, can bring about a considerable reduction in necessary ground transmitted power, this then represents a very real savings in terms of dollars. 2) It is desirable to make the "large user" satellite, such as any advanced versions of Telstar, Relay, Syncom, etc., accessible to ground stations having the ability to transmit less power than stations designed specifically for these satellites. 3) Future communications satellites will be designed for a "small user" system, e.g., where many small stations (those where ground station cost and complexity are limiting factors) participate in a world-wide communications network via an active communications satellite.

This report suggests that a reduction of necessary ground transmitted power in a communications satellite system can be accomplished quite easily by the reduction of the satellite front-end noise figure, using a tunnel diode amplifier as the low noise device. Traveling-wave tubes, parametric amplifiers and masers are compared with the tunnel diode as a means of reducing the satellite noise figure, in terms of weight, compactness, gain, noise figure, bandwidth and overall complexity.

Six low noise receivers using tunnel diodes as the RF amplifying elements were purchased by research personnel within Goddard Space Flight Center and were tested to determine the suitability of these devices for spacecraft usage. These receivers were designed for operation at room temperature; however, temperature tests were performed to determine which parts of the receivers were temperature sensitive. This report lists the test results and summarizes the general applicability of tunnel diode amplifiers to spacecraft use for the purpose of reducing the front-end noise figure.

## REDUCTION OF SATELLITE FRONT-END NOISE AS A MEANS OF REDUCING GROUND TRANSMITTED POWER

In seeking ways to reduce the large amount of signal power that must be transmitted from the ground to insure an acceptable carrier to noise ratio at the input to the ground receiver terminals, it is necessary to examine a typical active satellite microwave communications link. An examination of the expression for the carrier to noise ratio at the ground receiver terminals in terms of the system parameters may offer a clue to which parameters may be altered to keep the same carrier to noise ratio when the ground transmitted power is reduced. Consider the basic block diagram of a typical satellite microwave communications link shown in Figure 1.

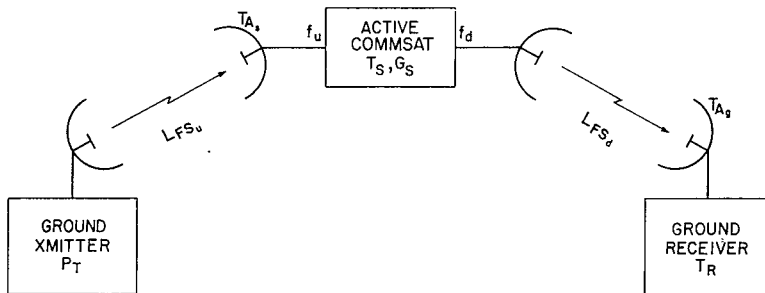


Figure 1

In determining the carrier to noise ratio at the ground receiver input terminals, a synchronous orbit is assumed for the satellite and the satellite antenna patterns are assumed to cover the earth only. The carrier power at the satellite

input terminals is equal to the ground transmitter power ( $P_T$ ) multiplied by the ratio of up-link antenna gain ( $G_{Au}$ ) to the free space path loss for the up-link ( $L_{FSu}$ ). This power ( $P_T G_{Au}/L_{FSu}$ ) is then amplified by the satellite electronic gain ( $G_s$ ) and retransmitted to the ground. The carrier power at the ground receiver terminals is then equal to the satellite transmitted power ( $P_T G_s G_{Au}/L_{FSu}$ ) multiplied by the ratio of down-link antenna gain ( $G_{Ad}$ ) to the free space path loss for the down-link ( $L_{FSd}$ ). The received carrier power is then

$$P_G = P_T \frac{G_s G_{Au} G_{Ad}}{L_{FSu} L_{FSd}} \quad (1)$$

The total effective noise power at the satellite input terminals is equal to the external noise added to the signal on the up-link due to black body radiation from the earth, plus the noise due to the effective noise temperature of the receiver referred to the input terminals of the receiver ( $k[T_A + T_S]B_s$ ). This noise power is then amplified by the satellite electronic gain, and retransmitted to the ground via the down-link. The noise power received at the ground receiver due to the up-link and satellite noise sources is then

$$N_{Gu} = k(T_A + T_S)B_s \frac{G_s G_{Ad}}{L_{FSd}} \quad (2)$$

Additional noise power is added on the down link because of the sky noise that the ground receiving antenna picks up plus the noise of the ground receiver referred to its input terminals. These are characterized by a ground receiver noise temperature  $T_G$ . The total noise at the input to the ground receiver terminals is then

$$N_G = N_{Gu} + N_{Gd} = k(T_A + T_S)B_s \frac{G_s G_{Ad}}{L_{FSd}} + k T_G B_s \quad (3)$$

Equations (1) and (2) enable the expression for the carrier to noise ratio at the ground receiver input terminals to be written as

$$\left(\frac{C}{N}\right)_G = \frac{P_G}{N_G} = P_T \frac{\frac{G_s G_{Au} G_{Ad}}{L_{FSu} L_{FSd}}}{kB_s \left[ (T_A + T_S) \frac{G_s G_{Ad}}{L_{FSd}} + T_G \right]} \quad (4)$$



This equation can be arranged in a more usable form by defining the following constants:

$$L_T(\text{db}) = G_{Au}(\text{db}) + G_{Ad}(\text{db}) - L_{FSu}(\text{db}) - L_{FSd}(\text{db})$$

$$L_d(\text{db}) = G_{Ad}(\text{db}) - L_{FSd}(\text{db})$$

Equation (4) now becomes:

$$\left(\frac{C}{N}\right)_G = P_T \frac{G_s}{L_T \left[ \frac{G_s}{L_d} (T_A + T_S) + T_G \right] k B_s} \quad (5)$$

At first glance, Equation (5) indicates that a fixed carrier to noise ratio can be maintained by first decreasing the ground transmitted power and then increasing the satellite electronic gain an equivalent amount in db. This can be assumed correct for the case where the ratio  $G_s/L_d$  in Equation (5) is so small as to make the up-link contribution to the total system noise very small. This reduction in ground transmitted power (and corresponding increase in satellite electronic gain) can continue, however, only until the carrier to noise ratio at the input to the satellite receiver becomes less than that needed to give the required carrier to noise ratio on the ground.

A reduction in the satellite front-end noise temperature reduces the up-link noise contribution, increasing therefore, the carrier to noise ratio at the satellite receiver input terminals. The maximum antenna noise temperature will be 300°K (due to the antenna beamwidth being that for full earth coverage only). Typical satellite receiver noise temperatures for present-day satellites are in the order of 2700°K.

This general consideration of a satellite microwave communication link then strongly suggests that reducing the satellite front-end noise figure enables the system designer to reduce the size of the ground transmitter or perhaps even the size of the ground antenna to some degree. A following section shows how a reduction of the noise figure of the ATS front-end results in a reduction of approximately 3 db in the required ground transmitted power.

## COMPARISON OF LOW NOISE RF AMPLIFIERS FOR SPACECRAFT APPLICATION

Having determined that the area showing the most promise of improving spacecraft noise performance is the reduction of the RF amplifier noise figure, an investigation of the various possible RF amplifiers becomes necessary. The devices to be considered here are traveling-wave tubes, parametric amplifiers, masers and tunnel diodes. These four devices characterize, in general, the variety of devices available for low noise amplification in the 1-10 Kmc region. A brief outline of the underlying theory is given, with a discussion of parameters of typical devices. A final comparison of the devices is given with respect to requirements for space communication.

### Traveling-Wave Tube

In a traveling-wave tube (TWT), an electron gun, operating at a very high accelerating potential, produces a beam of initially uniform-velocity electrons that pass through the helix to the collector (see Figure 2). A source of microwave energy connected to the input waveguide excites a wave that moves along the helix to the output waveguide. The helix exhibits the property that the waves tend to follow, with the velocity of light, the wire with which it is wound. In so doing, the waves produce a longitudinal component of the electric field on the axis of the helix, propagated axially with reduced velocity. Therefore, from the standpoint of the axial component of the electric field, the helix may be considered as a wave guide in which slow waves are propagated. For a typical 4 Gc tube operated with a beam-accelerating voltage of about 1500 volts, the electron velocity is slightly greater than  $1/13$  the speed of light. In order that the axial component of the field will be propagated with a velocity slightly less than that of the electrons, the ratio of the pitch of the helix to its diameter is chosen so that the total length of the wire approximates 13 times the helix length. Interaction of the longitudinal component of the electric field of the helix with the beam of electrons results in reduction of the average velocity of the electrons and in conversion of the kinetic energy lost by the electrons into microwave energy of the wave. The energy of the wave is delivered to the output termination through a matched junction.

The TWT has already found wide application in communication satellites, as a power tube, however, and not as low noise device. The inherently wide bandwidth and high gain of the TWT make it highly suitable for use as a satellite transmitter. For example, the Advanced Syncom satellite used a TWT that could deliver 5.5 watts power output at 4 Gc over a bandwidth of  $\pm 102.5$  Mc with a power gain of 37.4 db. Since the TWT in this case was used as the last stage

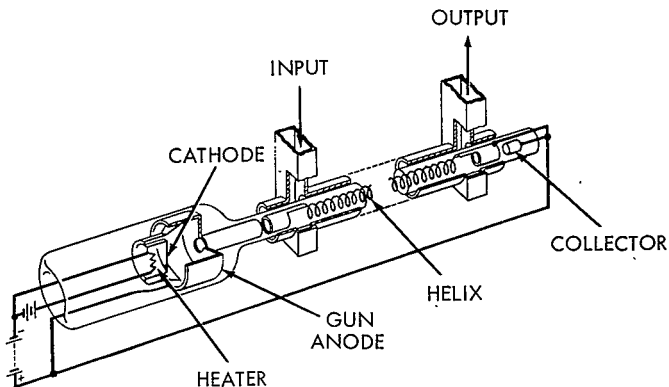


Figure 2

of a transponder, the noise figure was of little consequence. Hence, a tube was used with a noise figure of over 20 db. In addition, the tube required a cathode voltage of -1160 volts at 23.62 ma and a collector voltage of -600 v at 21.5 ma. The TWT in the satellite was 9 inches long and weighed 17.5 ounces without its power supply.

The requirements of a TWT as a low noise device are different than those of a power amplifier. It is generally desired that the noise figure of the tube be minimized and the gain kept as high as possible in order to overcome the noisiness of any following stages of amplification. The following tube parameters are those of an available low noise TWT: 4.5 db noise figure at 6 Gc with a 500 Mc bandwidth. Power out is 1/2 mw with 25-30 db gain. The TWT is approximately 4-1/2 inches in diameter and 12 inches long, and weighed approximately 17 pounds. The total d.c. power required is 7 watts.

It should be mentioned that cooling of the helix and refinements in the focusing and accelerating structures have lowered the noise figure of certain tubes to about 2.7 db. The expense of this reduced noise figure is a much larger tube and associated cooling apparatus, making this type of TWT unsuitable for spacecraft use.

## Parametric Amplifiers

The term parametric amplifier is associated with any amplifying or frequency-converting device which utilizes the properties of non-linear or time-varying reactances. The type of parametric amplifier of interest here uses the voltage sensitive capacitance of a semi-conductor diode to convert energy from a pump frequency  $f_p$  to a signal frequency  $f_s$  by interaction with another circuit tuned at an idler frequency  $f_i = (f_p - f_s)$ . The device presents a negative resistance input at the signal and idler frequencies and consequently can be used for amplification. It is a low-noise amplifier because, ideally, it is purely reactive and, therefore, no noise power is emitted. In practice, noise power is present in the signal and idler circuit.

In the simplest version, the pump frequency is chosen to be approximately twice the signal frequency so that the signal and idler frequencies are supported in one circuit. If the bandwidth of this tuned circuit is sufficiently large, the signal and idler frequencies need not be exactly the same so that the complications of the pumping at the correct phase do not arise. However, the noise figure of this amplifier will not be as good as for one in which the idler frequency is greater than the signal frequency. The former type of amplifier is sometimes referred to as a degenerate amplifier and the latter as a non-degenerate amplifier.

Negative resistance amplifiers are inherently unstable. One mode of operation of a parametric amplifier is up-converter operation in which the output frequency is the sum of the signal and pump frequencies. The power gain of this amplifier is the ratio of the output to the input frequency and the amplification is unconditionally stable. The disadvantage of this type of amplifier is that it requires a high pump frequency to achieve any useful gain.

Paramps have been widely used as low noise RF amplifiers in ground receiving systems and are second only to masers in low noise performance. Low-noise performance is being improved almost daily because of this wide usage and manufacturers offer a wide variety of paramp performance, depending upon the particular system requirements. Uncooled paramps are readily available in the neighborhood of 6 Gc, which have a noise figure of 3.2 db with a 20 db gain over a bandwidth of  $\pm 35$  Mc. The amplifier must be pumped at  $K_u$  band and weighs 5 lbs.

By cooling the semiconductor diode, the noise figure of the same paramp can be reduced to approximately 0.75 db while the gain and bandwidth remain essentially the same as for the uncooled case. The pump power required for both cases was 100 mw. The cost of this lower noise figure is the addition of a bulky cooling apparatus, which is undesirable for spacecraft use.

## Masers

Solid state maser operation, or microwave amplification by stimulated emission of radiation, makes use of the phenomena and techniques of electron paramagnetic resonance. A brief discussion of this phenomena and how it relates to solid state maser operation will be given here. Since the type of maser which most readily finds application in communications is the traveling-wave maser, only this type will be discussed and only performance figures for this type will be given.

The essential feature of a paramagnetic material is that it contains a large number of atoms or ions which individually possess permanent magnetic dipole moments. The common maser material ruby contains chromium  $C^{3+}$  ions, chromium being a member of the iron transition group and the  $C^{3+}$  ion having a permanent magnetic dipole moment. Magnetic atoms or their associated magnetic dipole moments are most commonly called spins. Quantum theory states that when a d-c magnetic field is applied to a ruby crystal, an atomic spin can take on only some one of four allowed orientations and allowed energies. Figure 3 shows the four allowed orientations and the four corresponding paramagnetic or Zeeman energy levels.

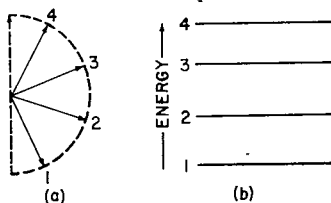


Figure 3

For typical magnetic fields of a few thousand oersteds, the spacing between Zeeman levels is  $10^{-5}$  electron volt which corresponds to transition frequencies in the microwave range. The population distribution of the spins among these four levels at thermal equilibrium is determinable by the Boltzman expression, which says that  $N_i/N_j = e^{-(E_i - E_j)/kT}$ . For a chosen d-c magnetic field strength, the relative populations of the levels may appear as in Figure 4, at thermal equilibrium.

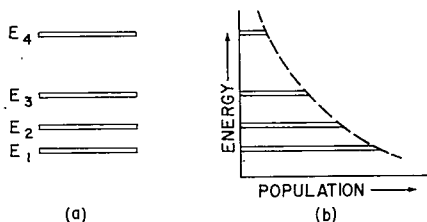


Figure 4

Although ruby and other materials may have four or more energy levels, only three are used in many maser schemes. If a relatively strong microwave signal at the transition frequency  $f_{31}$  is applied to the ruby crystal of Figure 4, more upward transitions will take place between levels 1 and 3 than downward transitions because there are more spins initially in level 1. As a result, the population of level 3 will begin to increase and that of level 1 will decrease until the populations are the same.

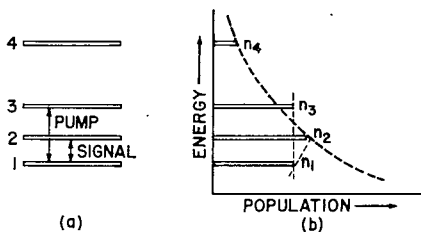


Figure 5.

Figure 5 shows the saturated condition of the 1-3 transition. The saturating radiation at  $f_{31}$  is called the pump frequency. The 1-2 transition now has a population inversion and if a weak signal at  $f_{21}$  is applied to the ruby crystal, it will be amplified by maser amplification. This occurs because the applied signal stimulates more downward than upward transitions between levels 1 and 2.

It is significant that the strength of the maser action in a maser crystal is proportional to the population difference between the two signal levels when the maser crystal is in the pumped condition. This difference is dependent on the crystal temperature and this temperature must be very low ( $4.2^{\circ}\text{K}$  or colder) for good maser operation. This requires, of course, some external cooling apparatus.

An excellent way to use this maser amplification property is to distribute the maser crystal along a length of transmission line. With pump power applied to the maser material in some fashion, the signal to be amplified is sent into one end of the transmission line. In effect, the transmission line has a negative attenuation per unit length and the signal amplifies with distance along the line. The amplified signal is then taken out at the far end of the transmission line. This type of device is called a traveling-wave maser.

An ultra-low-noise amplifier such as the solid-state maser is most useful in systems where other noise contributions in the system, including the background noise from the source, are correspondingly small. Masers have found application, therefore, in communication satellite ground receiver systems.

A ruby traveling-wave maser was developed for the Telstar Satellite Communications Experiment which is representative of masers now available. The maser operated at 4 Gc and was characterized by an average gain of approximately 35 db over a bandwidth of 25 Mc. An overall noise temperature of  $3.5^{\circ}\text{K}$  was achieved which closely approximates sky temperatures. The maser required a bath temperature of  $4.2^{\circ}\text{K}$ . The complete maser package including the liquid helium cooling apparatus was large enough to be rack mounted, thereby eliminating maser usage in a satellite.

### Tunnel Diode Amplifier

Tunnel diode amplifiers, like masers and parametric amplifiers, use a negative conductance effect to provide amplification. A tunnel diode consists of a semiconductor p-n junction using highly doped material, giving it a low series resistance and a characteristic as shown in Figure 6.

As seen from the curve, the diode displays a negative conductance in the region between 50 and 100 mv with a corresponding diode current of less than 10 ma. A circulator is used to separate the input of the amplifier from the following circuitry. The incoming signal is amplified by the negative resistance and then reflected to the output terminal of the circulator. (For a more detailed examination of the tunnel diode, see Appendix A.)

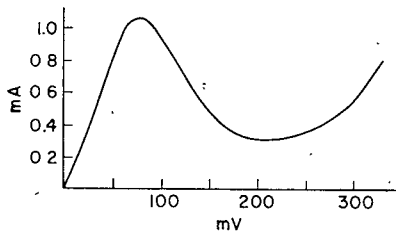


Figure 6

To date, tunnel diode amplifiers have not been widely used in communication circuitry although a need has existed. Tunnel diode amplifiers are readily available as "off-the-shelf" items throughout the frequency range of 1-10 Gc. Typical amplifiers weigh only 1/3 pound and require an input power of +10 vdc at 15 ma. A typical tunnel diode amplifier offers a noise figure of 4.5 db at 6 Gc with a gain of 18 db over a bandwidth of 500 Mc. No cooling apparatus or pumping is needed, making the dimensions of the amplifier quite small.

#### Comparison of Low-Noise Amplifiers

A comparison of low-noise microwave amplifying devices is given in Table 1.

Table 1

	TWT	Paramp	Maser	TD
Noise figure, db	4.5	3.2	0.05	4.5
Noise temperature, °K	550	320	3.5	550
Gain, db	25	20	35	18
Bandwidth, Mc	500	500	25	500
Cooling required	No	No	Yes	No
Pump required	No	Yes	Yes	No
Dimensions	Medium	Medium	Very Large	Small
Weight	Medium	Medium	Very Large	Small
Power supply	High	High	High	Low



It is immediately apparent that the maser, in spite of its ultra-low noise property, is unsuitable for spacecraft application because of the cooling requirement. The noise figure of the satellite RF amplifier, as previously shown, need not be far below 3 or 4 db because of the thermal noise contribution to the system by the earth. The low noise figure of the maser would then be wasted, in effect.

The choice then is between the TWT, parametric and tunnel diode amplifiers. Of the three, the parametric amplifier exhibits the lowest noise figure — over one db lower than the TWT and TD. The cost of this lower noise figure is the pumping required. This necessitates a separate microwave oscillator tube with its associated power supply. The power gain and bandwidths of the three amplifiers are approximately the same. The tunnel diode, however, requires less space, weighs far less and uses far less power to amplify.

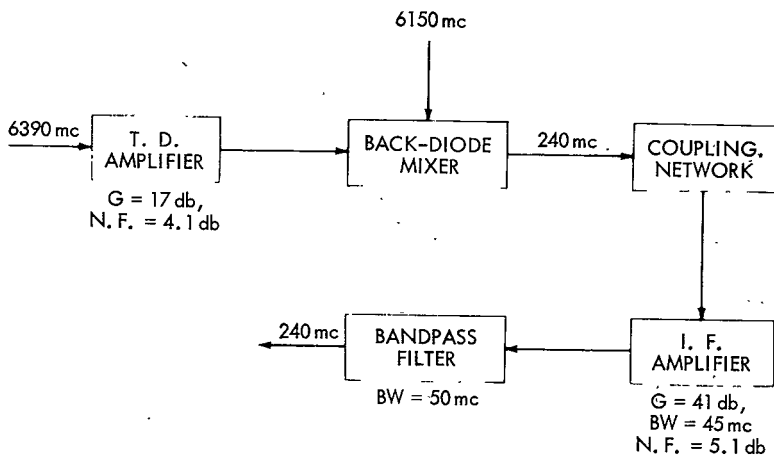
The tunnel diode amplifier is then the logical choice of a low noise amplifier to reduce the satellite front-end noise figure, making a reduction of ground transmitted power possible. The wide bandwidth of the tunnel diode amplifier is compatible with wideband signals used today and has sufficient gain to overcome the noisiness of the mixer to a large degree. It is lightweight and compact and would add no significant complexity to present day satellite front-ends. The only input power required is that used to bias the diode for operation in the negative resistance region.

## DESCRIPTION OF THE SIX LOW NOISE RECEIVERS

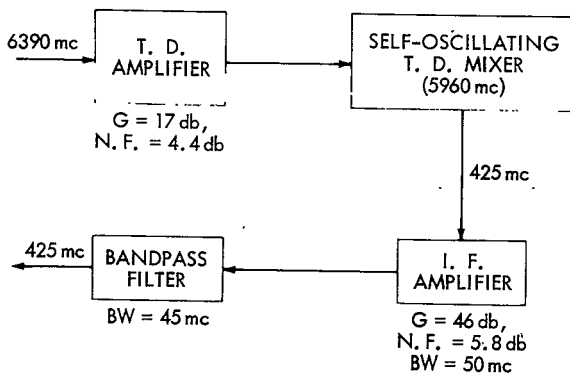
Six low noise receivers were purchased by Goddard Space Flight Center for the purpose of evaluating them with respect to usage in communications satellites. The six receivers were essentially "off-the-shelf" items designed for operation at room temperature.

Complete receivers, instead of just the tunnel diode amplifiers were bought to eliminate the problem of compatibility between the amplifiers and the following components. In general, the components are interchangeable. It was also desirable, as a secondary purpose, to observe the performance of different types of mixing devices. Consequently, back diodes, self-oscillating tunnel diodes, and resistive mixers are used in different receivers.

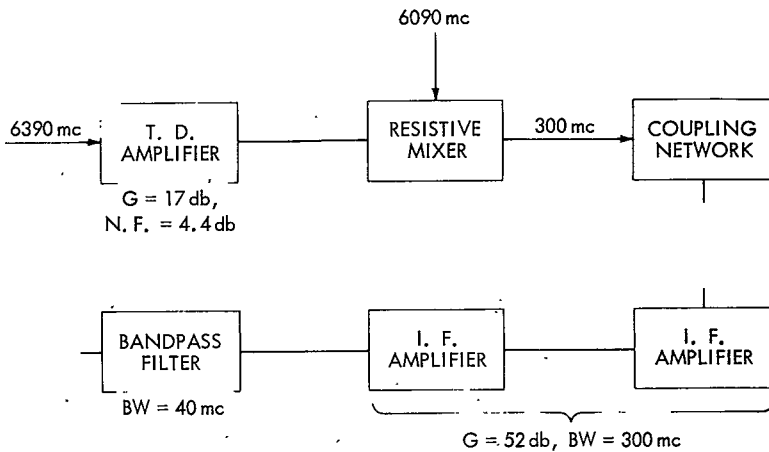
The six receivers are shown in block diagram form on the following pages.



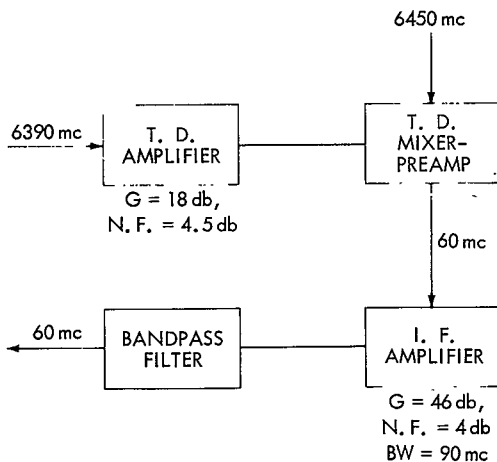
RECEIVER NO. 1



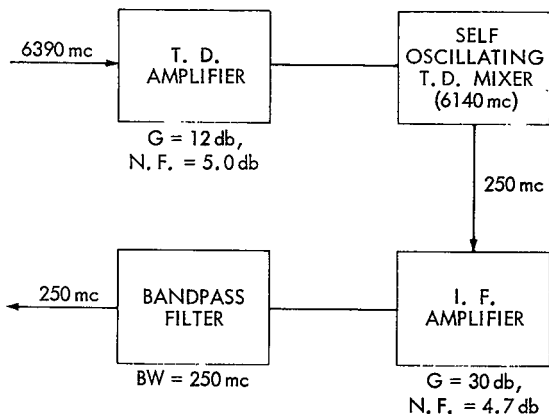
RECEIVER NO. 2



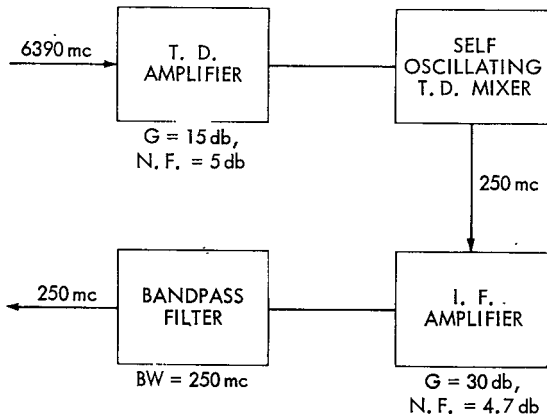
RECEIVER NO. 3



RECEIVER NO. 4



RECEIVER NO. 5



RECEIVER NO. 6

## TUNNEL DIODE RECEIVER PERFORMANCE TESTS

### Tunnel Diode Receiver Saturation Level

The saturation level of a receiver is defined as that input power level to the receiver which causes the gain of the receiver to drop off 1 db from the non-saturated gain. This level is determined by applying an RF signal, small enough to insure operation in the linear gain region of the tunnel diode receiver, to the input. The input power is increased in steps and the gain measured until the receiver operates in its saturated region.

More particularly, the signal generator output is fed to the input of the tunnel diode receiver through a calibrated precision variable attenuator and an RF single-pole, double-throw switch. The TD receiver output is fed through another switch, to the detector. The detector output is fed to the standing wave indicator. The receiver is bypassed when the switches are thrown to the calibration position.

The arrangement of test components for the receiver saturation test is shown in Figure 7.

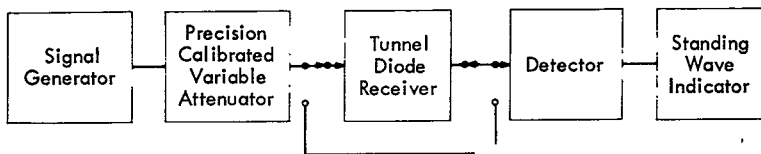


Figure 7

The test results show that the input power causing the receiver gain to deviate from linearity by -1db for the six tunnel diode receivers varied between -45 dbm and -81 dbm as shown in Figure 8. When the tunnel diode amplifiers were tested alone, the input power needed to saturate the six amplifiers varied between -35 dbm and -42 dbm, as seen in Figure 9. Obviously the IF amplifiers saturate before the tunnel diode amplifiers, decreasing the dynamic range of the amplifiers. The effect of temperature variation on the saturation levels of the amplifiers and receivers is discussed in the summary of test results at the end of the test section.

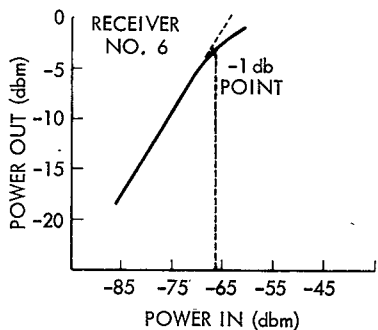
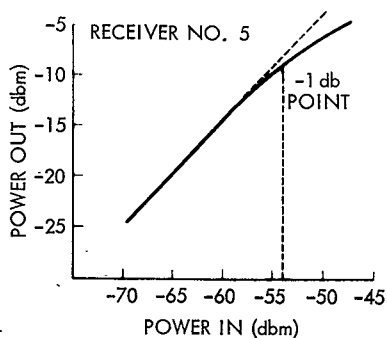
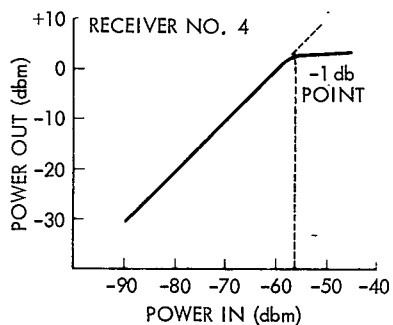
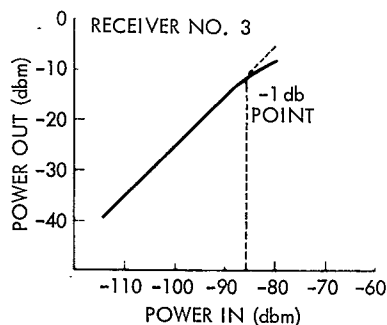
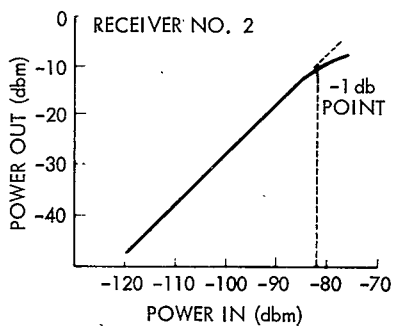
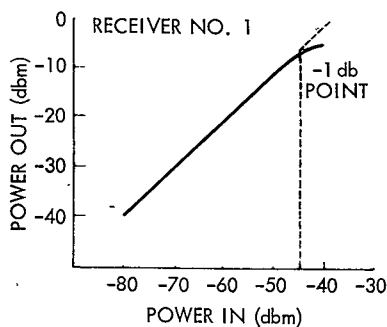


Figure 8

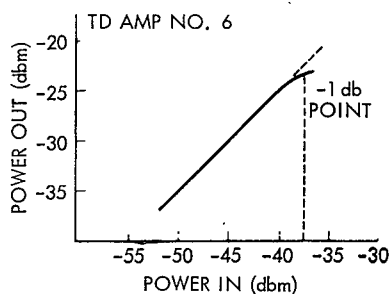
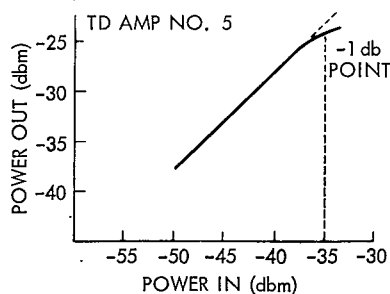
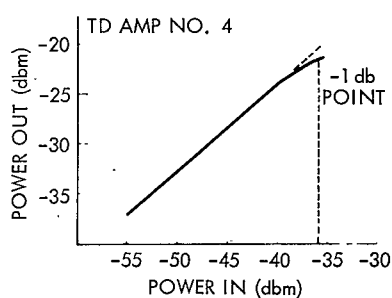
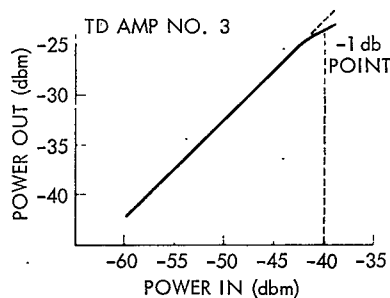
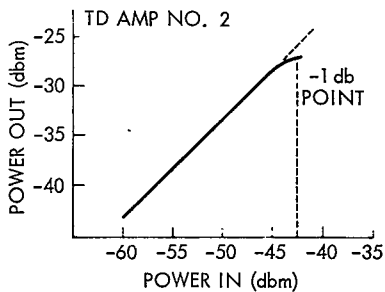
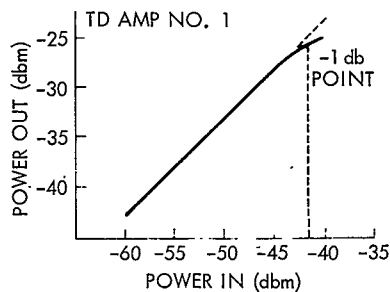


Figure 9

## Tunnel Diode Receiver Broadband Noise Figure

The purpose of this test is to determine the noise figure of the tunnel diode receiver over its bandwidth. The noise figure is defined as the ratio in db of the actual output noise power of the receiver to the noise power which would be available if the receiver were perfect and merely amplified the thermal noise of the input termination rather than contributing any noise of its own.

The automatic measurement of noise figure using a standard broadband noise source provides sufficient accuracy and permits continuous display of the noise figure as the receiver is optimized for noise performance. The output of a standard noise source providing 15.2 db excess noise is fed to the input of the tunnel diode receiver. The output of the receiver is fed into a mixer whose noise figure is known. The local oscillator frequency is adjusted so that the mixer output is centered in the passband of an IF amplifier which follows the mixer. The output of the IF amplifier is then applied to the input of an automatic noise figure meter.

Excess noise power added by the noise source is based on the effective fired temperature of the source. The argon gas discharge is 15.2 db above the reference temperature power. The total noise power output of the receiver with the noise source "off" is:

$$N_1 = GK T_0 B + RCVR$$

where G is the receiver power gain. Then the total noise power output of the receiver with the noise source "on" is:

$$N_2 = GK T_0 B + RCVR + Excess \times G$$

The noise factor is then:

$$F = \frac{(\text{total noise output from receiver})}{(\text{output power if noiselessly amplified})} = \frac{GK T_0 B + RCVR}{GK T_0 B}$$

The noise contributed by the receiver is then:

$$RCVR = (F - 1) GK T_0 B$$



The excess noise power from the gas discharge tube at the input is:

$$\text{Excess} = \frac{T_2 - T_0}{T_0}$$

Where  $T_2$  is the effective fired temperature of the noise source. The ratio at the output is then:

$$\frac{N_2}{N_1} = \frac{GK T_0 B + (F - 1) GK T_0 B + \frac{T_2 - T_0}{T_0} GK T_0 B}{GK T_0 B + (F - 1) GK T_0 B}$$

By substitution, it is found that:

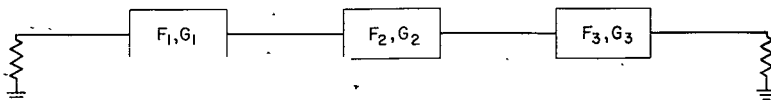
$$F = \frac{\frac{T_2 - T_0}{T_0}}{\frac{N_2 - N_1}{N_1}} \quad \text{or} \quad F_{db} = 10 \log_{10} \left( \frac{T_2}{T_0} - 1 \right) - 10 \log_{10} \left( \frac{N_2}{N_1} - 1 \right)$$

The first term is a function of the noise source and is known to be 15.2 db. The ratio then contains the noise figure information. The automatic noise figure meter measured this ratio and then displays the noise figures in db.

The arrangement of test components for the tunnel diode receiver broadband noise figure is shown in Figure 10.

The measurement of broadband noise figure as described in the procedure does not give the noise figure of the tunnel diode amplifier alone but of the TD amplifier-mixer-IF amplifier combination. To determine the noise figure of the TD amplifier alone the relationship between the noise figures of each of the devices and the total noise figure must be derived.

Consider three components in cascade with noise factors  $F_1$ ,  $F_2$ , and  $F_3$  and gains of  $G_1$ ,  $G_2$  and  $G_3$  respectively.



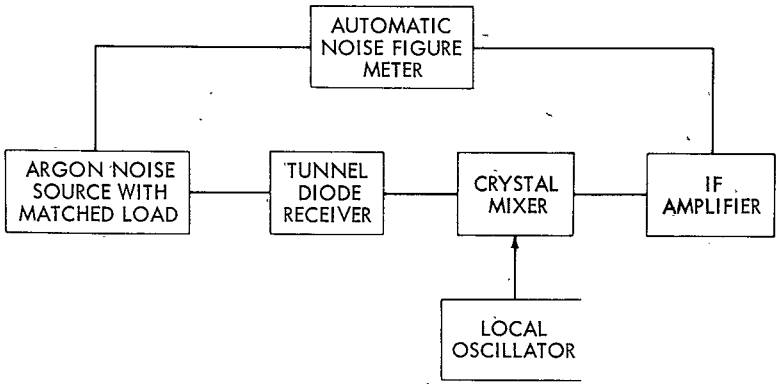


Figure 10

Assuming that the elements are matched and that the first-stage input is terminated in its matched impedance at  $T_0$ . The total noise factor of the three elements in cascade is defined as the ratio of the noise power out due to noisy amplification of the thermal noise supplied to the network by the input termination at  $T_0$ , to the noise power out due to noiseless amplification of the same input thermal noise.

$$\begin{aligned}
 &= \frac{G_1 G_2 G_3 K T_0 B + G_1 G_2 G_3 K T_1 B + G_2 G_3 K T_2 B + G_3 K T_3 B}{G_1 G_2 G_3 K T_0 B} \\
 &= 1 + \frac{T_1}{T_0} + \frac{1}{G_1} \frac{T_2}{T_0} + \frac{1}{G_1 G_2} \frac{T_3}{T_0}
 \end{aligned}$$

The quantity  $1 + T_1/T_0$  is simply the noise factor of the first component or  $F_1$ . The quantities  $T_2/T_0$  and  $T_3/T_0$  are simply equal to the noise factor of the second component minus one and the third component minus one, respectively. Therefore,

$$F_{\text{total}} = F_1 + \frac{F_2 - 1}{G_1} + \frac{F_3 - 1}{G_1 G_2}$$

The noise factor of the first stage is then given as

$$F_1 = F_{\text{total}} - \frac{(F_2 - 1)}{G_1} - \frac{(F_3 - 1)}{G_1 G_2}$$

In each measurement the effect of the mixer and IF amplifier was taken into account and the resulting tunnel diode amplifier noise figures are given in Table 2 below for 25°C. The noise figures of the six receivers are also given.

Table 2

Model	T.D. Amplifier	Overall Receiver
Receiver No. 1	4.2 db	4.9 db
Receiver No. 2	4.5 db	5.0 db
Receiver No. 3	4.5 db	4.9 db
Receiver No. 4	4.6 db	5.0 db
Receiver No. 5	5.0 db	6.4 db
Receiver No. 6	5.0 db	6.5 db

The variation of the noise figures with temperature is discussed in the summary of test results at the end of the test section.

#### Tunnel Diode Receiver Small Signal Gain vs Frequency

The purpose of this test is to determine the small signal gain of the receiver as the frequency of the input signal is varied. An RF signal, small enough to insure operation in the linear gain region of the tunnel diode receiver, is applied to the input. The ratio of output to input power represents the small signal gain of the receiver. This is done at frequency intervals over the RF bandwidth of the receiver.

The arrangement of components for this test is shown in Figure 11. The signal generator output is fed into the input of the tunnel diode receiver through a precision calibrated variable attenuator and an RF single-pole double-throw switch. The TD receiver output is fed through another RF switch to a detector. The output of the detector is fed to the standing wave indicator. The TD receiver is bypassed when the switches are thrown to the calibration position.

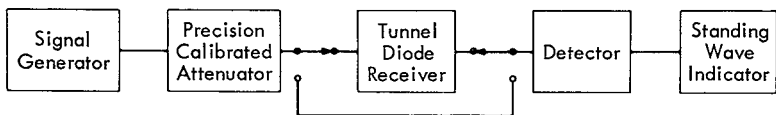


Figure 11

The data showing the variation of small signal gain with frequencies for the six different receivers is plotted in Figure 12. The bandwidths of the six receivers are approximately determined by the bandpass filters at the output of the IF amplifiers. The data showing the variation of small signal gain with frequency for the six different tunnel diode amplifiers is plotted in Figure 13. The amplifier bandwidths are approximately determined by the circulators used with the tunnel diodes.

The variation of both receiver and amplifier small signal gain vs frequency with temperature is discussed in the summary of test results at the end of the test section.

## ANALYSIS OF TEST RESULTS

### Tests at +25°C

The original purpose of the tests was to determine whether or not tunnel diode receivers now available could improve communication satellite system performance by reducing the noise temperature of the satellite front end. It has been shown that the carrier to noise ratio at the ground receiver is directly proportional to the ground transmitter power and to the satellite electronic gain but is effected very little by the effective noise temperature of the spacecraft input terminals. Therefore, as the satellite electronic gain is increased the ground transmitted power can be decreased accordingly. It has also been shown, however, that the ground transmitter power can only be decreased to a minimum level before the combined thermal noise of the up-link and the receiver becomes greater than the received signal at the receiver. Hence, an improvement in the effective noise temperature of the spacecraft input terminals, means that a lower signal can be detected. As was pointed out in a previous section of this report, there is no need to improve the front-end noise figure to any value below 3 db because the spacecraft antenna "sees" the earth at 300°K.

With this background review, the results of the tests should determine, in general, whether or not a tunnel diode receiver can enable the ground transmitted

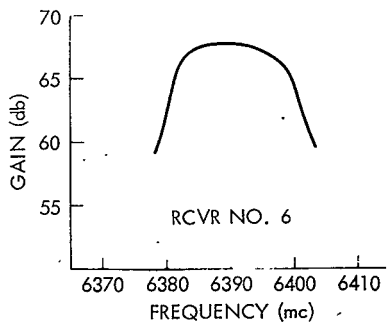
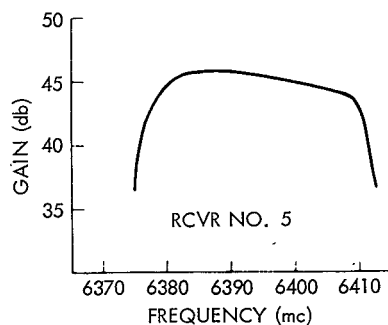
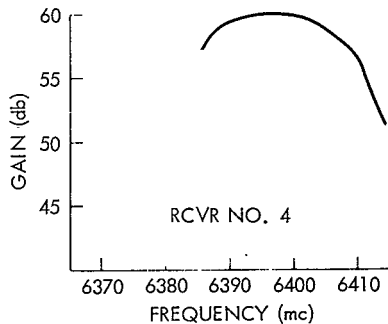
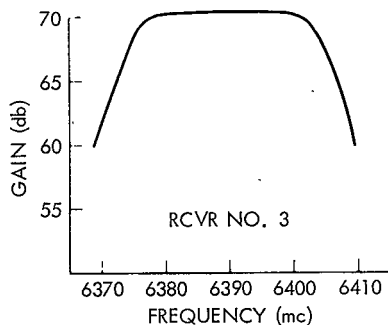
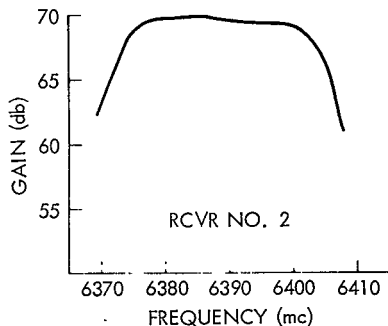
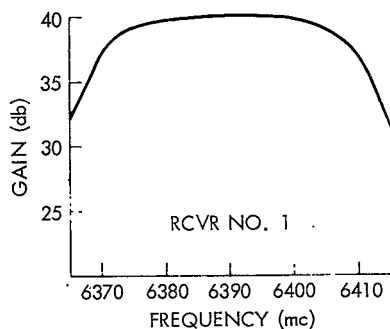


Figure 12

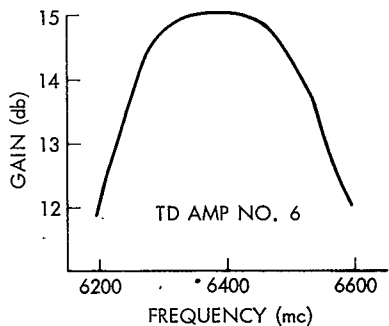
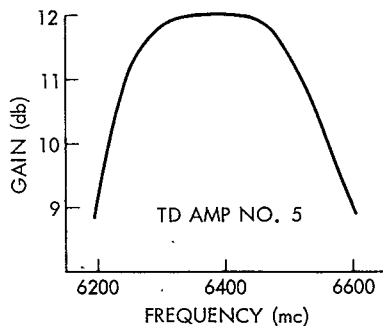
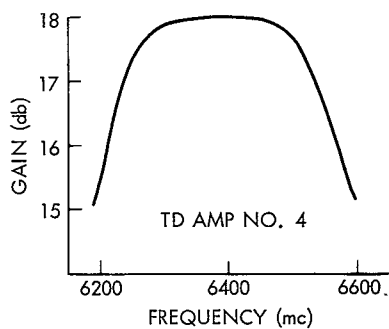
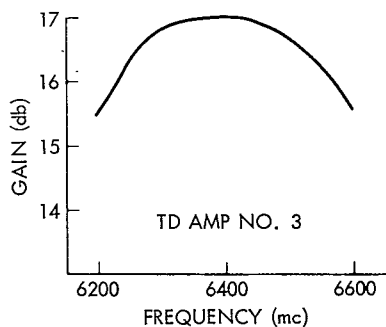
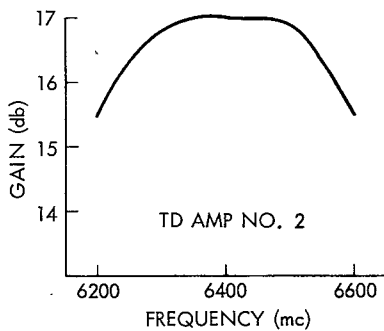
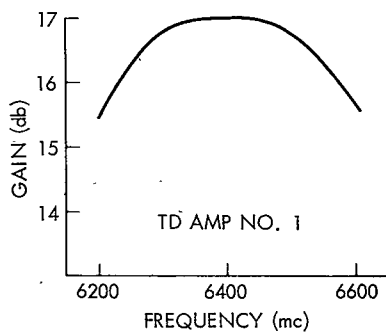


Figure 13

power to be reduced (with all the obvious technical and economic advantages) by raising the satellite electronic gain and reducing the front-end noise contribution.

The measurement of broadband noise figure of the receivers and tunnel diode amplifiers alone indicates that a considerable improvement over conventional satellite front-ends having a noise figure of 10 db, is readily provided. With any of the TD receivers or with any of the TD amplifiers preceding a conventional mixer, it appears that the ground transmitter power for existing communication satellites could be reduced by more than 3 db. The measurement of small signal gain indicates that any of the TD amplifiers could supply the necessary increase in satellite electronic gain to offset the decrease in ground transmitter power made possible by the reduction in front-end noise figure. The gain vs bandwidth data also showed that the tunnel diode amplifiers are certainly wide-band devices, the smallest bandwidth of the six amplifiers being 200 mc. The saturation tests showed the TD amplifiers to be capable of handling typical received powers of -20 to -60 db. Receivers 2, 3 and 6 might possibly saturate, however, if typical received powers were fed into them.

### Temperature Tests

As was mentioned in the introduction to this report, the six tunnel diode receivers were purchased for operation at room temperature. No temperature specifications other than operation at room temperature were given to the manufacturers of the receivers. It was decided, however, to test the receivers at the two temperature extremes that the electronics package on the Applications Technology Satellite would be exposed to in orbit (+50°C and -10°C). From this limited environmental testing it was hoped that if the receiver performance was degraded by this temperature variation, the cause of the degradation could be found.

The temperature extremes did not cause any breakdown or failure of the tunnel diodes themselves or of the mixer or IF amplifiers. The receiver and tunnel diode amplifier performance was, however, degraded in every test by the temperature variations. This degradation has been attributed to the adverse effect of temperature variation upon the ferrite material of the circulator used in each of the tunnel diode amplifiers. The effect is in general due to a change in isolation and shifting of the isolation vs frequency curve with temperature changes.

The effects of the isolator instability on the performance of the TD amplifiers and receivers is discussed below. The data was quite erratic; therefore, no performance curves are given, merely trends in performance.

The broadband noise figure of each of the tunnel diode amplifiers increased when measured at +50°C and -10°C. The noise figure varied from 2 to 4 db above that at room temperature and on certain occasions the tunnel diode amplifier would go into oscillation. The increase in noise temperature and the occasional oscillation is attributed to the mismatch between the tunnel diode and the following circuitry caused by the change in isolation of the circulator. The small signal gain decreased in every instance, and dropped to 30 db below the gain at room temperature for the worst case. The cause of this is a combination of mismatch due to the change in isolation and a change in the bandwidth of the circulator. The power input required to saturate the amplifiers also decreased with temperature change, thereby decreasing the dynamic range.

These temperature test results should not be interpreted as necessarily indicating an inability of the tunnel diode receiver to function properly in an orbital environment. As previously stated, the variations were attributed to the isolator performance, the temperature characteristics for which were not specified to the manufacturers. With proper ferrite design, the circulator instability with temperature variation can be eliminated and the performance of the receiver becomes essentially the same as at room temperature. Considering this, a tunnel diode receiver shows great promise as a means of improving existing communication satellite system performance by enabling reduction of ground transmitter power.

## APPLICATION OF TUNNEL DIODES TO A SATELLITE SYSTEM

Equally as important as presenting the data from the analysis of individual tunnel diode receivers is their possible application to a satellite system. In order to make any qualifying statements as to possible application, a proposed system of interest will first be discussed. The system will be that of the Applications Technology Satellite (ATS). Emphasis will be placed on the ATS front end for use as the example.

The component of interest here is the input mixer. Stripline circuitry is employed for all signal path and a 3 db etched circuit ring hybrid is employed for introducing the received signal and local oscillator signal. Glass diodes are utilized to develop the 60 mc IF difference signal which is coupled out through RF chokes to an OSSM output connector. The mixer introduces 6.5 db loss at a 9.0 db noise figure. It is the intent then of this section to replace the mixer of the ATS system with a tunnel diode amplifier and matched mixer to show the overall improvement in the system by analytical methods.



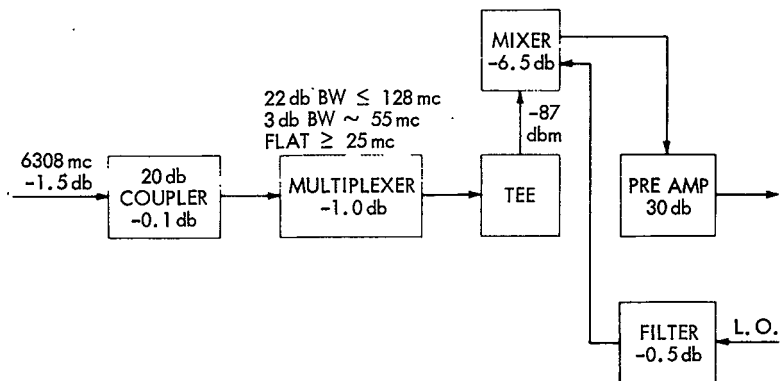


Figure 14—Block Diagram of ATS System of Interest

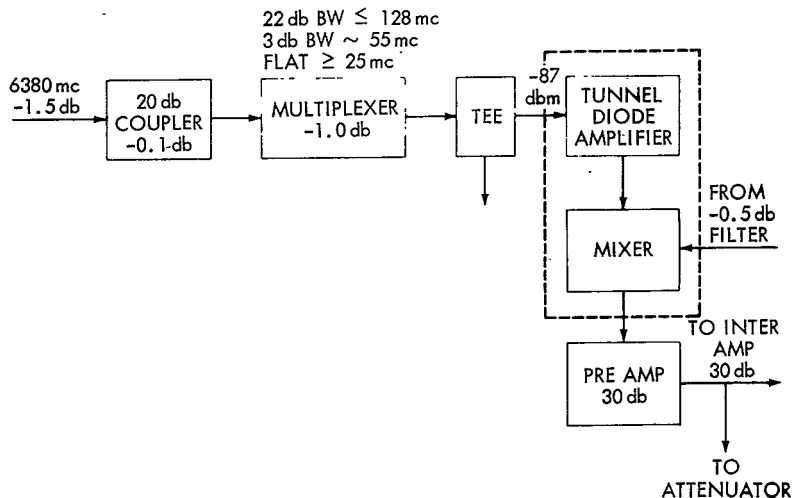


Figure 15—Block Diagram of Possible Tunnel Diode Application on the ATS Front End

The application shown in Figure 15 will replace the mixer stage with a tunnel diode amplifier and matched mixer. The improvement in this case from a 9 db noise figure and a 6.5 db loss to a 12 to 18 db gain at a 4 db noise figure. The gain would be a function of the device bandwidth with gain bandwidth products ranging from  $4.1 \times 10^9$  at 6 Gc for one product and  $0.8 \times 10^9$  to  $2.9 \times 10^9$  range from 2 Gc to 7 Gc for the other product.

The improvement can be shown from the following analytical analysis by substituting the tunnel diode amplifier for the ATS mixer.

The information to follow was obtained from GSFC Requirements Specification, ATS Experimental Communications System Description and Requirements, SS&P Division.

The example is just one possible improvement obtained by using tunnel diodes.

Table 1  
Ground-to-Satellite SSB Multiple Access Mode  
85-foot Antennas, 600 Two-Way Channels, Phased Array

Transmitter Peak Power . . . . .	DBM <u>70.0</u>
Transmitter Average Power . . . . .	DBM <u>61.0</u>
Loading Factor . . . . .	DB <u>12.8</u>
Channel Test Tone Power . . . . .	DB <u>48.2</u>
Diplexer Loss . . . . .	DB <u>-1.0</u>
Grid Antenna Gain . . . . .	DB <u>62.1</u>
Space Attenuation . . . . .	DB <u>-200.8</u>
Receiving Antenna Gain . . . . .	DB <u>8.0</u>
Off Beam Center Allowance . . . . .	DB <u>-1.5</u>
Diplexer and Miscellaneous Losses . . . . .	DB <u>-3.0</u>
Received Test Tone Power . . . . .	DB <u>-88.0</u>
Receiver Noise Figure . . . . .	DB <u>9.0</u>
Receiver Noise Power Density . . . . .	DBM/cps <u>-164.4</u>
Channel Bandwidth (3.1 kc) . . . . .	DB <u>34.9</u>
Psophometric Noise Weighting Factor . . . . .	DB <u>-2.5</u>

Table 3 (continued)

Receiver Channel Noise (WGTD) . . . . .	DBM <u>-132.0</u>
Test tone/Fluctuation Noise (WGTD) . . . . .	DB <u>44.0</u>
Test tone/Intermod Noise (WGTD) . . . . .	DB <u>47.0</u>
Test tone/Weighted Noise . . . . .	DB <u>42.3</u>

By this substitution of the tunnel diode the term that changes is the receiver noise power density.

$$NF = 1 + \frac{T_e}{290}$$

NF = noise figure of the system

$T_e$  = System temperature

$$T = (NF - 1) 290$$

$$NF = 10 \log_{10} N, NF \approx 4 \text{ db}$$

$$N = 10^4 = 2.5$$

$$T = (2.5 - 1) 290 = 435^\circ K$$

Receiver noise power density is given by

$$N = KT \text{ DBM/CPS}$$

$$K = 1.38 \times 10^{-23} = -198.6 \text{ DBM}$$

$$T = 435^\circ K = 26.4 \text{ db}$$

$$N = -172.2 \text{ dbm/cps}$$

This is an improvement over the previous noise power density of 164.4, or 7.8 db.

Receiver Channel Noise (WGTD) Goes to -139.8 dbm

Since assuming the other parameters remain constant the Test tone/Fluctuation Noise (WGTD) now changes to +139.8 -88.0 = 51.8 db. This is the 7.8 improvement over 44.0 db.

The 7.8 db can not be subtracted directly from the transmitter power since the Test Tone/Fluctuation Noise (WGTD) is a function of the Test Tone/Intermod. Noise (WGTD). The difference between them should be 3.2 db. Thus;

TT/Fluctuation Noise 51.8 db

TT/Inter Mod. Noise (WGTD) . . . . . 47.0 db

For every 1db in TT/fluctuation noise and transmitter power there is a -2db decrease in the TT/Inter Mod. Noise (WGTD). This then modifies the signal to noise ratio to

TT/Fluctuation Noise. . . . . 49.1 db

TT/Inter Mod. Noise . . . . . 51.8 db

There is an improvement in the transmitter average power of 2.7 db.  
(Almost cuts power in half.) Or,

$$10 \log_{10} P = \text{db}$$

$$32.1 \text{ db} = 10 \log_{10} P$$

$$P = 10^{3.21} \text{ watts}$$

$$\underline{P = 1.6 \text{ kilowatts}}$$

with the tunnel diode

$$29.4 \text{ db} = 10 \log_{10} P$$

$$P = 10^{2.94}$$

$$\underline{P = .86 \text{ kilowatts}}$$

an improvement of 1.6 -.86k watts of .74k watts. (Decrease in Required Power).

This is just one example of possible system improvement using a tunnel diode front end.

Another consideration would be holding all elements constant. The difference between the 6,000 mile orbit and the synchronous orbit in path loss is 8.2 db maximum. The improvement in the front end could account for all but 0.4db of this increase.

#### ACKNOWLEDGMENT

The authors wish to express their appreciation to George M. Orr for his assistance in selecting the tunnel diode receivers that were evaluated during the program.

## APPENDIX A

### THE TUNNEL DIODE AS A CIRCUIT ELEMENT

#### INTRODUCTION

The "tunnel diode" is a heavily doped semiconductor diode which exhibits a negative resistance characteristic over a small voltage range in the forward-biased direction. This negative resistance generated in the p-n junction is a source of energy released only by the stimulus of an electrical signal which is then enhanced by that energy. Signal gain, or amplification, is the result of this effect. The negative resistance can also be used for such functions as power generation, frequency conversion, switching and signal detection.

In looking at the noise properties of the tunnel diode to determine its sensitivity to weak signals, it is recognized that the electrical noise has two sources. The first is Johnson noise which has for its origin the thermally excited particles of the bulk-material. Quantitatively, this is the thermal noise of the effective series resistance of the diode. The second is shot noise which arises through the use of bias current. It has been fairly well determined that the shot noise is the limiting factor in usefulness of the tunnel diode as low noise preamplifier.

#### I. The Tunnelling Effect

The basic materials used in a typical p-n junction type diodes are chemically pure semiconductors of very low conductivity, such as germanium and silicon (Group IV) and the compounds gallium-arsenide and indium antimonide (Groups III-V). To make p or n type materials, impurity or doping atoms must be added by controlled insertion to give a typical impurity density of  $10^{15}$  atoms/cc for conventional diodes and an impurity density  $10^4$  times as large for tunnel diodes. Conduction then takes place by the relative motion of positively and negatively charged carriers - by electrons in n-type materials and by holes in p-type material.

The p-n junction is an internal boundary between p-type and n-type material within a single crystal. Because of the difference in impurity types on the two sides of the junction, a narrow, electrically charged dipole region is formed at the junction. This is caused by impurity atoms which have gained (or lost) an electron. This transfer of electrons constitutes a current flow, but (under zero

bias condition) the requirement for thermal equilibrium dictates that the net current be zero. Hence, the dipole region gives rise to a potential barrier at the junction which prevents any net current. The width of the dipole region depends on several things such as donor and acceptor concentrations, applied voltage, and the dielectric constant of the semiconductor material. The width increases for increases in dielectric constant or applied voltage and decreases for increases in donor or acceptor concentrations.

The energies which an electron in a crystal can possess fall into certain bands of "allowed" energy levels, separated by "forbidden" energy bands. Each level corresponds to a number of quantum states all having the energy of that level. In a semiconductor, the two allowed bands of interest in p-n junction theory are the valence band and the conduction band. The separation of these two bands is called the energy gap,  $E_g$ , and is the forbidden band.

In a material which is a good insulator, the conduction band is completely empty and the valence band is completely filled. That is, all available states in the conduction band are empty. A completely filled or completely empty band does not conduct current. If, however, the material is doped p-type, then some of the states in the valence band are vacated, leaving a deficiency of electrons in this band and allowing movement of carriers, and hence a current can flow. Similarly, if the material can be doped n-type, there will appear electrons in the lower energy states of the heretofore empty conduction band. These electrons are also free to move about in the crystal, and hence a current can flow.

If a p-n junction is formed the energy band structure is deformed or bent in the dipole region, the deformation being due to the potential step formed across the dipole region. A typical energy diagram of a p-n junction in equilibrium is shown in Figure A-1 below.

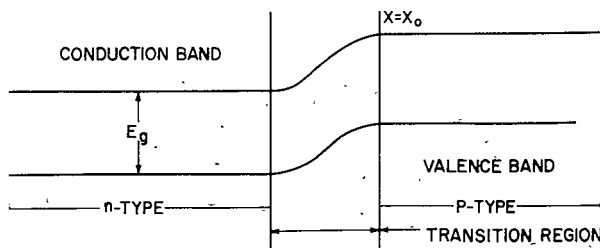


Figure A-1

If a forward bias is applied to the p-n junction shown in Figure A-1, free electrons in the conduction band of the n-type material can receive sufficient energy to cross the junction into the conduction band of the p-type material. In other words, the majority carriers receive sufficient energy from an applied source to overcome the potential barrier and cause an external current to flow in the circuit. The probability that any electrons in the conduction band of the n-type material go into the valence band of the p-type material is zero because of the high energy gap or forbidden gap.

In the tunnel diode, which can have an impurity or dopant level  $10^4$  times higher in both p and n-type materials in regular diodes, the transition region is much narrower, ( $100\text{\AA}$ ). A typical energy diagram of a p-n junction where both regions are highly doped is shown in Figure A-2 below.

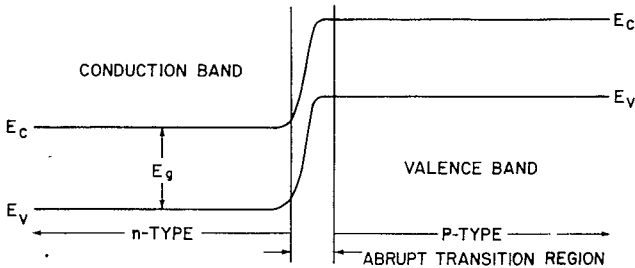


Figure A-2

When a small forward bias is applied to the p-n junction shown in Figure A-2, the electrons of the conduction band of the n-type material do not gain enough energy to climb the potential barrier into the conduction band of the p-type material. It is seen from Figure A-2 that there are energy states of the same level in both the conduction band of the n-type material and the valence band of the p-type material. The probability that electrons in the conduction band of the n-type pass through or "tunnel" into the valence band of the p-type material is now finite instead of zero, because of the very narrow forbidden gap. This electron movement (and corresponding hole movement in the opposite direction) causes a current to flow in the external circuitry. This "tunnelling current" increases with increase in bias to a "peak" value and then decreases to a minimum or "Valley." This occurs because the energies of the electrons in conduction band of the n-type material are raised by the applied bias to levels that have few corresponding vacant levels in the valence band of the p-type material. Finally,



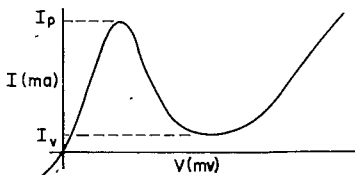


Figure A-3

the majority electrons receive sufficient energy from increased bias to overcome the potential barrier and go into the conduction band of the p-type material. This represents normal diode action of the higher values of bias voltage. The well-known I-V curve of the tunnel diode is shown in Figure A-3.

## II. The Tunnel Diode Equivalent Circuit

The fundamental equivalent circuit for the tunnel diode as depicted in Figure A-4 has been shown by Sommers and others to be well representative of the actual physical arrangement of the tunnel diode when biased at a point typified by point A in Figure A-5.

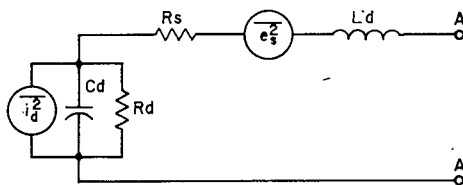


Figure A-4

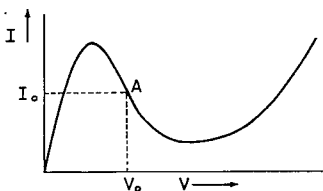


Figure A-5

$R_s$  and  $L_d$  constitute the series parasitic impedance which accompanies any physically realizable device.  $L_d$  is the lead inductance and  $R_s$  is the resistive loss of the leads and the spreading resistance of the junction itself.  $C_d$  is the junction capacitance. The two generators  $e_s^2$  and  $i_d^2$  represent the internal noise of the diode.  $e_s^2$  is the mean-squared noise voltage generated by thermally induced noise currents in

the parasitic resistance  $R_s$ .  $i_d^2$  is the mean-squared value of the noise current contributed by the dc bias current through shot effect.

In order to understand fully the interaction of all the diode characteristics in a practical tunnel diode circuit, one must convert the impedance and generators to either a single series loop or a single parallel nodal form.

Series Form – Figure A-6 represents the series form of the tunnel diode equivalent circuit.

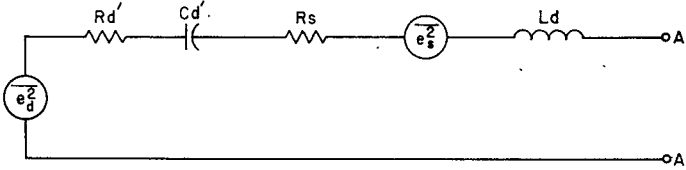


Figure A-6

The values of  $R_s$ ,  $L_d$ , and  $e_s^2$  are the same as those shown in Figure A-4. Converting  $C_d$  and  $R_d$  to a series impedance, it is found that

$$R_d' = \frac{R_d}{1 + Q_d^2} \quad (A-1)$$

$$C_d' = \frac{C_d (1 + Q_d^2)}{Q_d^2} \quad (A-2)$$

$$Q_d = \omega R_d C_d \quad (A-3)$$

where  $e_d^2$  is the equivalent mean-squared noise voltage due to dc bias shot effect, and may be found by applying Thevenin's theorem to the junction components of Figure A-4. Therefore

$$\overline{e_d^2} = \frac{i_d^2 R_d^2}{1 + Q_d^2} \quad (A-4)$$

and from equation (A-1)

$$\overline{ed^2} = \overline{id^2} R_d R_d' \quad (\text{A-5})$$

Parallel Form – The series circuit of Figure A-6 can be transformed into the parallel form as shown in Figure A-7.

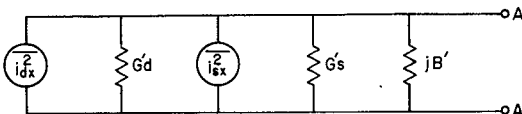


Figure A-7

$G_d$  is the conductance component between the terminals A-A which is due to the junction resistance  $R_d$ .  $G_s$  is the Conductance component between the A-A terminals which is due to the parasitic resistance  $R_s$ . The susceptance  $jB$  is that shunt equivalent susceptance between terminals A-A which is due to the combined effects of  $C_d$  and  $L_d$ . Let

$$jX = j\omega L_d - \frac{j}{\omega C_d'} = j \left( \omega L_d - \frac{Q_d^2}{\omega C_d (1 + Q_d^2)} \right)$$

The actual  $Q$  of the complete diode, including parasitic elements is then

$$Q' = \frac{x}{R_d' + R_s}$$

Transforming  $R_d + R_s$ , and  $X$  by the usual series to parallel transformations,

$$G_s' + G_d' = \frac{1}{(R_d' + R_s) (1 + Q'^2)} \quad (\text{A-6})$$

and

$$jB' = \frac{-Q}{(R_d' + R_s) (1 + Q'^2)} \quad (\text{A-7})$$

Since the series and parallel equivalent circuits' represent the same device, the losses in each are identical, and to satisfy such a condition it can be shown that the ratio of loss conductance to junction conductance ( $G_s/G_d$ ) of Figure A-7 must equal the ratio of loss resistance to junction resistance ( $R_s/R_d$ ) of Figure A-6. That is,

$$\frac{G_s'}{G_d'} = \frac{R_s}{R_d'}$$

Therefore,

$$G_d' = \frac{1}{(R_d') \left(1 + \frac{R_s}{R_d'}\right)^2 (1 + Q'^2)} \quad (A-8)$$

$$G_s' = \frac{R_s/R_d'}{R_d' \left(1 + \frac{R_s}{R_d'}\right)^2 (1 + Q'^2)} \quad (A-9)$$

$i_{dx}^2$  is the value of the equivalent mean-squared noise current generator between the terminals A-A which is contributed by the dc bias through shot effect.  $i_{sx}^2$  is the mean-squared value of the equivalent noise current generator between terminals A-A being contributed by thermal excitation in the loss conductance  $G_s$ . Both  $i_{dx}$  and  $i_{sx}$  may be found by the application of Norton's theorem for equivalent constant current generators to the circuit of Figure A-7. This gives,

$$\overline{i_{dx}^2} = \frac{\overline{ed^2}}{(R_d' + R_s)^2 (1 + Q'^2)} \quad (A-10)$$

or

$$\overline{i_{dx}^2} = \overline{ed^2} \frac{G_d'}{R_d'}, \quad (G_d' \neq 1/R_d') \quad (A-11)$$

and,

$$\overline{i_{sx}^2} = \frac{\overline{es^2}}{(R_d' + R_s)^2 (1 + Q'^2)} \quad (A-12)$$

or

$$\overline{i_{sx}^2} = e s^2 \frac{G s'}{R_s} \quad (A-13)$$

### III. The Negative Resistance Amplifier

There are two basic configurations in which a tunnel diode may be used as a negative resistance amplifier. The first is the transmission type amplifier in which the negative resistance element is placed between the signal source and the load immittance in such a way as to modify the immittance "seen" by the source and hence increase the signal transferred to the load. If no isolators or circulators are used, the circuit is completely bilateral, and also reflective if stable. By reflective it is meant that, although large transmission gain is achieved, there is a large reflected wave (amplified signal) traveling back toward the source. In addition, if noise in the load is treated as a signal, it is found that there appears in the load a large amplified load noise component which tends to drastically limit the minimum noise figure which can be attained.

The second configuration is the reflection type amplifier. The reflection type amplifier makes use of the large reflected component to which reference was made in the above statements about the transmission amplifier. In the construction of the reflection type amplifier, one encounters the problem of separation of the weak incident (input) signal from the larger reflected (output) signal. This separation of waves is usually accomplished by the use of a circulator. If the ports are arranged in a ring, then there is an arrangement such that if a signal enters any given port, it will be coupled with low loss out the adjacent port, either in the clockwise or counterclockwise sense, but in the same sense for all ports. The coupling to the adjacent port in the opposite sense and any other port will be greatly attenuated.

The use of the circulator to separate the signals as described is satisfactory from the viewpoint of circuit operation; however, the expense of a circulator, its size and weight, and the requirement of the magnetic field are some of the many arguments presented by those who seek a different solution. An alternative method is the use of a coupled transmission line, 3 db directional coupler in conjunction with two balanced reflection type amplifiers to perform the operation of signal separation.

Only the reflection type amplifier with circulator isolation will be considered here as the six tunnel diode receivers tested all used this type of amplifier.

Reflection Type Amplifier with Circulator Isolation - The problem of stability as a result of impedance inconstancy is handled easiest at the higher frequencies by the use of a circulator. Only the basic circuits are to be considered.

### a. Series tuned amplifier

If the amplifier is to be series tuned, a reactance equal to  $-X$  must be placed in series with the diode as shown in Figure A-8.

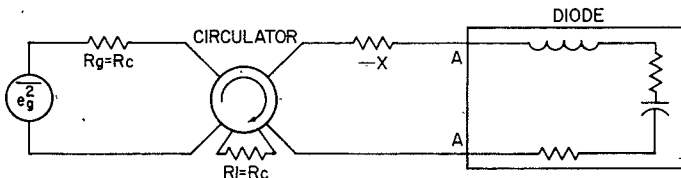


Figure A-8

The circulator and the transmission lines used have characteristic impedance  $R_c$  the source (generator) impedance is  $R_g = R_c$  and the load impedance is  $R_l = R_c$ .

For stability in a series circuit, the total real part of the loop impedance must be positive. This means that  $(R_c + R_s)$  ( $R_d$ ) where  $R_d$  is the negative resistance in the series equivalent circuit.

Since the square of the reflection coefficient  $|\Gamma|^2$  is the reflection power gain,  $W_p$ , it may be written

$$W_p = |\Gamma|^2 = \left| \frac{(R_s + R_d') - R_c}{(R_s + R_d') + R_c} \right|^2 \quad (A-14)$$

In determining the bandwidth, it is found that  $B = \omega/Q$  where  $\omega$  is the center band angular frequency and  $Q = X/R_t$ . The usual range of operation is well below the resonant frequency of the unit, hence the relation  $X = 1 - X + \omega L_d$  must be used.

$$2\pi B = \frac{\omega (R_d' + R_s + R_c)}{\frac{Qd^2}{\omega C d (1 + Qd^2)}} \quad (A-15)$$

and by rearranging

$$2\pi B = \frac{1}{|R_d| C_d} \left( \frac{1-a}{a} \right) \left( 1 - \frac{Ks}{|R_d'|} \right) \cdot (\text{rad/sec}) \quad (\text{A-16})$$

where

$$a = \frac{|R_s + R_d'|}{R_c} \quad (\text{A-17})$$

Since all the noise voltages act about a common loop, the noise Figure, F, may be written as

$$F = \frac{\sum e k^2}{e g^2}$$

where

$$\overline{e g^2} = 4k T_0 B R_c$$

$T_0$  = temperature of the source impedance in degrees Kelvin. This gives

$$F = 1 + \frac{T}{T_0} \left[ \frac{\frac{G_{eq}}{G_d} R_d' + R_s}{R_c} \right] \quad (\text{A-18})$$

#### b. Parallel tuned amplifier

If the amplifier is to be parallel tuned, a susceptance equal to  $-B$  is placed in shunt with the diode as shown in Figure A-9.

The circulator and transmission lines used have characteristic conductance  $G_c$ ; the source (generator) conductance is  $G_g = G_c$ ; and the load conductance is  $G_l = G_c$ .

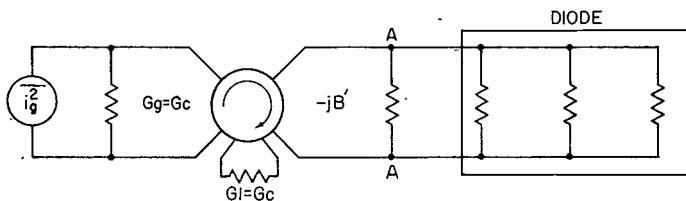


Figure A-9

For stability in a shunt tuned circuit, the total real part of the admittance must be positive. This means that  $(G_c + G_s) > |G_d|$ , where  $G_d$  is the negative conductance transformed from the junction.

Since the square of the reflection coefficient  $|\Gamma|^2$  is the reflection power gain,  $\mathbb{W}_p$ , it may be written

$$\mathbb{W}_p = |\Gamma|^2 = \left| \frac{G_c - (G'_d + G'_s)}{G_c + (G'_d + G'_s)} \right|^2 \quad (\text{A-19})$$

The bandwidth is again given by the relation for single tuned circuits;  $2\pi B = \omega/Q$ , where  $Q = B''/G_T$ . Since the below resonance condition is used, the tuning susceptance is inductive. This is combined with the series inductance and then the  $B''$  that is actually used is again only that due to the junction capacitance, and

$$B = \frac{\omega (G'_d + G'_s + G_c)}{B''} \quad (\text{A-20})$$

where

$$B'' = \frac{Q_d^2 / \omega C_d (1 + Q_d^2)}{(R'_d + R_s)^2 + (1 + Q'^2)} \quad (\text{A-21})$$

The bandwidth of the shunt tuned amplifier is then

$$2\pi B = \frac{1}{|R'_d| C_d} \left( \frac{1 - a}{a} \right) \left( 1 - \frac{G'_s}{|G'_d|} \right) (\text{rad/sec}) \quad (\text{A-22})$$



where

$$a = \frac{|G'_d + G'_s|}{G_c} \quad (\text{A-23})$$

As all of the noise currents act across a common admittance, the noise figure may be written as

$$F = \frac{\sum \overline{i_k^2}}{\overline{i_g^2}}$$

where

$$\overline{i_g^2} = 4k T_0 B G_g$$

$T_0$  = temperature of the source conductance in degrees Kelvin. This gives

$$F = 1 + \frac{T}{T_0} \left[ \frac{\frac{G_{eg}}{G_d} G'_d + G'_s}{G_c} \right] \quad (\text{A-24})$$

APPENDIX B  
THE EFFECT OF TEMPERATURE VARIATION  
ON FERRITE CIRCULATOR OPERATION

The performance of circulators, isolators, phase shifters, switches and other ferrite devices strongly depends upon the magnetic properties of the ferrite material used in the device. These magnetic properties, in general, are functions of the absolute temperature of the ferrite material. Thus, if a ferrite device is not specifically designed to operate in a varying temperature environment, the magnetic properties vary with temperature and device performance is altered considerably at times.

The following paragraphs discuss: (1) The principles of microwave-ferrite interaction; (2) The operation of Wye-type ferrite circulators; and, (3) The effects of temperature variation on Wye-type ferrite circulator operation.

I. Microwave-Ferrite Interaction

Ferrimagnetism - An atom consists of a nucleus and several electrons arranged in shells about the nucleus, each electron behaving as a tiny charge, spinning on its own axis. This spinning electric charge creates its own magnetic field of a definite direction. Since these magnetic fields tend to align themselves opposite to other magnetic fields, the direction is denoted as either "spin up" or "spin down." When two electrons align themselves so that their spins are in opposite directions their magnetic fields cancel.

The electrons of an atom are arranged in shells around the nucleus. Each shell permits an equal number of positions for electrons with spin up and with spin down. If the shell is completely filled, there is no net magnetic field. Certain atoms do not have completely filled inner shells, and the electron spins in the unfilled shells tend to be strongly unpaired. This lack of complete pairing causes relatively strong magnetic fields and the atom is said to have a strong magnetic moment. Iron, cobalt and nickel are examples of materials exhibiting large magnetic moments.

In ferr o magnetic materials, the atoms are so closely spaced that the magnetic field of one atom interacts with the magnetic field of its neighbor so that all the atoms in a small cell will spontaneously align themselves in the same direction. In ferr i magnetic materials, not all the atoms in a cell line up spontaneously; some line up antiparallel thereby decreasing the magnetic field.

Properties of Ferrite Materials – The spinning electron may be considered as a spinning mass which is charged electrically and is similar in many respects to the classical mechanical gyroscope. The d-c magnetic forces acting on the magnetic dipole are comparable to the gravitational force acting on a mechanical top.

If the spinning electron is regarded as a magnetic top, it is known that the magnetic moment of the electron precesses around the d-c magnetic field axis (or vector). It can be shown that the equation of motion of this magnetization vector is

$$\frac{d\vec{P}}{dt} = \gamma (\vec{H} \times \vec{P}) \quad (B-1)$$

where  $\gamma$  is the gyromagnetic ratio, defined as minus the ratio of the angular momentum to the magnetic moment of the electron. By analogy to the equation of motion of the angular-momentum vector of a mechanical top, it is seen that

$$\omega_0 = \gamma H \quad (B-2)$$

is the natural precession frequency of a magnetic dipole in a constant magnetic field.

When an r-f magnetic field is applied perpendicular to the d-c field, it is possible to transfer energy relatively efficiently from the microwave field to the system of spins if the resonance condition is satisfied, i.e., the driving frequency equals the natural precession frequency,  $\omega = \omega_0$ . This is explained by noting that the effect of adding an in phase component of torque to the precessional motion of the magnetic dipole under the influence of the constant magnetic field in the steady state condition, is an increase in the precession. This increase in precession occurs as energy is absorbed from the microwave field. At a value of the driving frequency not equal to the resonant frequency, the absorption occurs, but at a lower efficiency.

If an r-f magnetic field is applied to the ferrite and the d-c magnetic field is varied, the material will resonate at some value of  $H$ . The width of the

resonant absorption curve, in oersteds, measured at the point where the absorption in db is one-half the maximum absorption is called the resonance line width,  $\Delta H$ .

When a homogeneous ferrite specimen is placed in a uniform magnetic field, the medium becomes polarized. The magnetic dipoles induced at the surface by the applied field will create a component of magnetic field opposing the applied field. The total demagnetization is constant, regardless of the shape of the ferrite and the sum of the demagnetization factors in the three coordinate directions is given by

$$N_x + N_y + N_z = 4\pi \quad (B-3)$$

This effect must be taken into account when expressing the resonance condition, making equation (B-2)

$$\omega_0 = \gamma \left\{ [H_A - (N_z - N_x) M_s] [H_A - (N_z - N_y) M_s] \right\}^{1/2} \quad (B-4)$$

where  $H_A$  = applied steady magnetic field in oersteds in the  $z$  direction.

$M_s$  = saturation magnetization of the material

and

$$(N_x + N_y + N_z) = 4\pi$$

### Operation of Wye-type Ferrite Circulators

Circular Description - A circulator is a three- (or four-) port device in which energy introduced at one port circulates only to a second port while energy introduced at the second port is connected to the first port is isolated from the second port. This device is used to great advantage in reflection-type amplifiers such as the tunnel diode amplifier, where it is necessary to separate the input circuitry from the output circuitry and vice versa. The Wye-type circulator can be built either in waveguide or in strip-line.

When used in a tunnel-diode amplifier configuration it is desirable that the circulator have four ports. In this case two three-port devices are coupled together as shown in Figure B-1.

The input signal is introduced into port 1 where it circulates to port 2 where the tunnel-diode module is connected. Upon being reflected from port 2 the signal

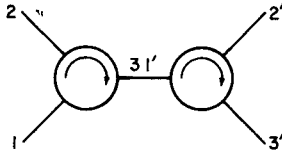


Figure B-1

enters port 3 (1'') and circulates to the output port at 2'. Any reflection from the output back into the circulator will rotate to port 3' where a matched load is used to absorb this reflected energy. In this fashion, the output is isolated from the input.

Circulation – Until very recently, the W-type circulators have been developed empirically and explained on a phenomenological basis in terms of the scattering-matrix technique. Qualitative explanations suggesting that the device requires both nonreciprocal scattering from a ferrite post and nonreciprocal field displacement within the ferrite have been advanced. These two notions are equivalent and correct, in principle, but they do not provide quantitative design information. The latter has now been furnished by Bosna, who has carried out an analytical solution of the electromagnetic boundary-value problem for the strip-line Wye-type circulator. His method of solution is used to explain the circulation mechanism briefly, as follows:

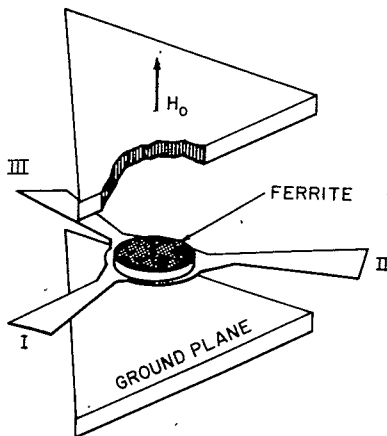


Figure B-2

The wave incident at port I is the fundamental mode with the r-f electric vector polarized parallel to the direction of the applied magnetic field. Thus, the ferrite disk supports two typical electromagnetic modes characteristics of such a tensor magnetic medium. Two mutually orthogonal components of the r-f magnetic field are excited in the plane perpendicular to the d-c magnetic field vector, i.e., the plane parallel to the broad face of the disk. One mode has a right-hand circularly polarized r-f magnetic vector and has increasing field intensities toward the right side of the input port. The other mode has the opposite sense of rotation. The combination of these two modes has a hyperbolic transverse electric field dependence. The plane wave incident at the input strip-line port is distorted within the ferrite so that the field intensities increase toward the region between input port I and output port II. This combination of the two sets of rotating modes computed by Bosna produces a wave pattern which has its field-displacement peak between the input and output ports and a null at the isolated port.

#### Effects of Temperature Variation on Circulator Operation

In general a number of ferrite characteristics or parameters are a function of temperature and each affects ferrite circulator performance to a greater or lesser degree. In addition to ferrite effects, circulator performance is also affected by any temperature dependency of the biasing magnets used. These parameters and their behavior with temperature change will be listed below, followed by a brief description of how the effects of temperature variation may be compensated for.

**Saturization Magnetization** – The maximum field that can be induced in a ferrite is defined as the saturization magnetization. The ferrite consists of molecules having large magnetic moments and spontaneously align themselves either parallel or anti-parallel with each other to produce a net magnetic moment. When the ferrite is heated, molecular motion within the material increases and tends to upset the alignment of the magnetic moments with a corresponding reduction in saturization magnetization.

It is recalled that the expression for the resonant frequency of the ferrite is a function of the saturization magnetization and therefore changes with temperature. A change in the resonant frequency of the ferrite piece affects the interaction between the electromagnetic radiation and the ferrite, which in turn would change the isolation and pass band of the circulator.

**Resonance Linewidth** – The resonant linewidth of the ferrite is the width of the resonance absorption curve of the ferrite, in oersteds, measured at the point

where the absorption in db is one-half the maximum absorption. As the temperature of the ferrite is lowered, the resonance linewidth increases, and the bandwidth of the ferrite device increases. This, in general, degrades the maximum isolation of the device.

Permeability - The permeability of a ferrite is a strong function of the temperature of the ferrite and of the applied magnetic field. In general, changes in saturation magnetization largely mask the effect of change in permeability.

Temperature Effect on Biasing Magnets - Any variation in the magnetization of the biasing magnets with temperature directly effects the dc magnetic field applied to the ferrite. This in turn alters the resonant frequency of the device and changes the frequency at which the microwave-ferrite interaction occurs.

Temperature Compensation - In a large number of cases, ferrite device performance in a varying temperature environment can be maximized by properly shaping the ferrite specimen used in the device. It is recalled that the equation for the resonant frequency of the ferrite is a function of the "demagnetization factors" of the ferrite. Rewriting equation B-4:

$$f = \gamma \left\{ [H_A - (N_z - N_x) M_s] [H_A - (N_z - N_y) M_s] \right\}^{1/2}$$

If the ferrite is shaped so that  $N_z - N_x = 0$  and  $N_z - N_y = 0$ , the resonant frequency no longer is a function of the saturation magnetization. This implies symmetrical shapes such as spheroids and triangles. If it is not practical to do the latter, the configuration should be such that  $(N_z - N_x)$  and  $(N_z - N_y)$  are equal and opposite.

Another possible method of compensation is "shunting," or keeping the resonant frequency of the ferrite constant when the saturation magnetization changes, by changing the value of the applied dc field accordingly. As  $M_s$  usually decreases with temperature, the resonant frequency increases with temperature. This can be compensated for by reducing  $H_A$  as temperature increases. The applied field can be reduced by placing a piece of temperature-sensitive steel in series with the magnet. The permeability of the steel decreases with increasing temperature, and  $H_A$  is reduced.

One additional consideration in compensating ferrites for temperature variation is the importance of selecting the proper chemical composition of the ferrite. A proper selection of ferrite material can often be achieved by analysis of printed data on the materials.

54. *Lepidochelys*